Romanian Reports in Physics **69**, 604 (2017)

PHOTOPHYSICAL STUDIES ON BIOCOMPOSITES BASED ON CARBON NANOTUBES AND CHLOROPHYLL-LOADED BIOMIMETIC MEMBRANES

M.E. BARBINTA-PATRASCU[1], N. BADEA[2], C. UNGUREANU[2], C. PIRVU[2], V. IFTIMIE[3], S. ANTOHE[1,4]*

[1]University of Bucharest, Faculty of Physics, Department of Electricity, Solid-State Physics and Biophysics, 405 Atomistilor Street, PO Box MG-11, Bucharest-Magurele, 077125, Romania, E-mail: elipatras@gmail.com, santohe@solid.fizica.unibuc.ro, s_antohe@yahoo.com
[2]"Politehnica" University of Bucharest, Faculty of Applied Chemistry and Materials Science 1-7, Polizu Str., 011061, Bucharest, Romania,
E-mail: nicoleta.badea@gmail.com, ungureanucamelia@gmail.com, c_pirvu@chim.upb.ro
[3]"Gh. Ruset Roznovanu" Technological High School, Roznov, Piatra Neamt, Romania,
E-mail: vioift@yahoo.com
[4]Academy of Romanian Scientists, 54 Splaiul Independentei, Bucharest, Romania,
E-mail: santohe@solid.fizica.unibuc.ro, s_antohe@yahoo.com
* *Corresponding author*: santohe@solid.fizica.unibuc.ro, s_antohe@yahoo.com

Received February 15, 2016

Abstract. A simple bottom-up strategy was used to achieve biocomposites designed from carbon nanotubes decorated with chlorophyll *a* – loaded biomimetic membranes. The emission fluorescence of chlorophyll a was exploited for monitoring insertion of quercetin in these biohybrids. Morphological aspects of the samples were revealed by AFM analysis. The bio-based composites obtained from multilamellar lipid vesicles, exhibited enhanced antioxidant activity (85%) and high antimicrobial properties against *Staphylococcus aureus* bacteria (area of inhibition zone was 143 mm^2). These findings open up new perspectives for biomedical applications of these biocomposites, as multifunctional scaffolds to carry therapeutic agents.

Key words: chlorophyll *a*, quercetin, biomimetic membranes, biocomposites, carbon nanotubes.

1. INTRODUCTION

The biohybrid nanomaterials are in the spotlight of the nanosciences, because they combine the characteristics of the components, giving rise to enhanced properties. One of the most interesting building block to design hybrid materials are carbon nanotubes (CNTs) that are allotropes of carbon, consisting of graphene layers (honeycomb networks of sp^2-hybridized carbon atoms) rolled-up into cylindrical structures. They are considered quasi-monodimensional materials due to their tubular shape with nano-scaled diameter and micrometric length. Based on

the number of graphene sheets, CNTs are divided into two main classes: single-walled carbon nanotubes (SWCNTs) and multi-walled carbon nanotubes (MWCNTs). SWCNTs are unique materials largely used to build drug delivery systems for biomedical purposes, due to their sp^2 hybridization surface and their large surface area, as compared to MWCNTs, therefore they can be charged with high amounts of drugs. Thus, nanocomposites based on SWCNTs and doxorubicin were achieved by Ciobotaru and co-workers, through covalent functionalization in order to use them as chemotherapeutic agents to treat breast cancer [1]. An other research team [2] prepared flavonoids-carbon nanotubes biohybrids, with high antioxidant capacity. On the other hand, hybrids of CNTs with porphyrins and porphyrin-like molecules could be integrated in novel photovoltaic devices and light-harvesting systems [3, 4].

The dispersion of SWCNT in biological media give rise to novel composite materials with improved properties. Thus, biofunctionalization of CNTs with bio-inspired membranes (liposomes) may be an effective method of increasing the biocompatibility of the nanotubes, resulting in bionanocomposites for biomedical applications [5, 6]. Liposomes are hollow vesicles containing two or more lipid bilayers separated by aqueous compartments; they are useful tools in biomedical field, because their architecture allows the incorporation of hydrophilic (in the aqueous compartments) and hydrophobic (inside of membranes) therapeutic agents. In addition, the structure of their lipid bilayers is similar to that of living cells. All these features make the liposomes to be used for various purposes. Thus, Badran reported the preparation of liposomes able to transdermal deliver higher amount of flufenamic acid, an anti-inflammatory drug [7]. Ang and her research team [8] created a bioelectronic platform using a graphene lipid bilayer interface for sensing biomolecules.

This work is a continuation of the scientific studies of our team [5, 6, 9, 10] in order to design biocomposites with novel interesting properties. Present paper describes a simple method to achieve biocomposites consisting of carbon nanotubes and chlorophyll-loaded biomimetic membranes. Chlorophyll *a* (Chl*a*), a photo-active porphyrin [11, 12], was used to label the artificial lipid bilayers in order to monitor the insertion of quercetin (*3,3′,4′,5,7-pentahydroxyflavone*), which is a very common flavonoid widely occurred in many plants (apples, onions, olives, apple skin, broccoli, red wine, tea, *Ginkgo biloba* etc.). It is well known that quercetin possess a broad spectrum of bio-applications: reduction of tumour incidence, anti-inflammatory, antioxidant and antiviral activities, prevention of platelet aggregation and of apoptosis induction, photo-oxidative stress suppression [13–16].

The obtained biocomposites were characterized by modern biophysical methods: emission spectroscopy, AFM analysis, chemiluminescence and antimicrobial investigation.

2. MATERIALS AND METHODS

2.1. MATERIALS

KH_2PO_4, Na_2HPO_4, luminol (5-amino-2,3-dihydro-phthalazine-1,4-dione), Tris (hydroxymethylaminomethane base), HCl, H_2O_2, peptone, DMSO (dimethyl sulfoxide) and the organic solvents of analytical grade (chloroform, ethanol, petroleum ether, methanol, n-propanol) were purchased from Merck (Germany). Quercetin (*3,3',4',5,7-pentahydroxyflavone*), NaCl, SWCNTs and DPPC (dipalmitoyl phosphatidylcholine) were supplied from Sigma Aldrich (Germany). The yeast extract was obtained from Biolife and the agar from Fluka.

Chlorophyll *a* (Chl*a*) was extracted in our lab, from fresh spinach leaves according the method of Strain and Svec [11].

All reagents were of analytical grade and all solutions were prepared using purified water (conductivity ≤ 0.1 $\mu S \cdot cm^{-1}$) from a Millipore Milli-Q system (USA).

2.2. SAMPLE PREPARATION

Preparation of biomimetic membranes. Multilamellar lipid vesicles (MLVs) were obtained by mechanical stirring (VIBRAX stirrer – OHIO 43230 USA, 200 rpm, 40 min) of a Chl*a*-DPPC thin film hydrated with a phosphate buffer (PB, KH_2PO_4–Na_2HPO_4) at physiological pH (7.4). Small unilamellar vesicles (SUVs) were prepared from MLVs, by ultrasound treatment (Hielscher Ti probe sonicator, UP 100 H - Hielscher Ultrasonics GmbH, 14513 Teltow, Germany).

Preparation of SWCNTs/liposomes (0.9 mg/mL) *biocomposites.* Two types of biocomposites (MLVs/CNTs and SUVs/ CNTs) were obtained by ultrasonic dispersion of SWCNTs in liposomal suspensions of MLVs and SUVs, respectively. The sample abbreviations used in this study are presented in Table 1.

Table 1

The sample abbreviation

Sample	Code
MLVs	TP1
SUVs	TP2
MLVs/CNTs hybrid	TP3
SUVs/ CNTs hybrid	TP4

2.3. CHARACTERIZATION METHODS

Testing of antioxidant capacity of the samples was achieved by chemiluminescence assay, on a Chemiluminometer Turner Design TD 20/20 (USA), using the free radical generator system containing: luminol (1 mM), H_2O_2 (10 μM)

in Tris-HCl buffer solution (pH 8.6). The *in vitro* antioxidant activity (AA%) of each sample was estimated by the equation:

$$AA = [(I_0 – I)/ I_0] \cdot 100\%, \quad (1)$$

where I_0 is the maximum CL intensity at t = 5 s, for the reaction mixture without the sample, and I is the maximum CL intensity for each sample at t = 5 s [17, 18].

The antibacterial activity was tested against *Staphylococcus aureus* ATCC 25923 bacterium, which was grown in Luria Bertani Agar (LBA) plates at 37 °C with the medium composition containing: peptone (10 g/L), yeast extract (5 g/L), NaCl (5 g/L) and agar (20 g/L); the stock culture was kept at 4 °C. The agar disc diffusion method [5, 19] was used and the experiments were performed in triplicate. The antimicrobial activity was evaluated by measuring the size of area of inhibition zone (A_{IZ}, mm^2) as a clear, distinct zone of inhibition surrounding the agar wells.

The fluorescence emission spectra of Chl*a* in samples were collected in the wavelength range of 600–750 nm, on a LS55 Perkin Elmer fluorescence spectrometer, by illuminating the samples with 430 nm excitation light.

The surface of the samples was analyzed using an APE Research A100-SGS (Italy) atomic force microscope (AFM), working in contact mode system. AFM images were processed with Gwyddion software.

3. RESULTS AND DISCUSSIONS

3.1. MORPHOLOGICAL ASPECTS OF THE SAMPLES

AFM images (Fig. 1) revealed morphological features in height and 3-D representation of the samples obtained in this work. Spherical and quasi-spherical lipid vesicles MLVs (Fig. 1a, sample TP1) and SUVs (Fig. 1b, sample TP2) were obtained through thin film hydration method. In contrast to the liposomes TP2 which possess nano-scaled size, with a mean diameter less than 300 nm, the lipid vesicles TP1 have larger diameters and are more agglomerated than TP2. Biofunctionalization of SWCNTs with MLVs biomimetic membranes (TP1) resulted in entities more uniformly distributed (Fig. 1c, sample TP3), opposite to SUVs-CNTs biocomposites which presents lower dispersion degree (Fig. 1d, sample TP4).

3.2. ANTIOXIDANT PROPERTIES OF THE SAMPLES

In order to establish the antioxidant capacity of the samples, a free radical generator system based on H_2O_2 in alkaline buffer solution (TRIS-HCl pH 8.6) was

used to mimic an *in vitro* oxidative stress. Luminol, a light amplifier in this system, increased the detection sensitivity of the activated oxygen species.

As could be seen in Fig. 2, all the samples presented antioxidant properties. The antioxidant activity of MLV liposomes increased from 67% (for TP1) to 85% (for TP3) after CNT addition, while the AA% value for SUV liposomes enhanced from 50% (for TP2) to 70% (for TP4) after CNT addition. This fact is explained by the ability of carbon nanotubes to scavenge free radicals due to their high electron affinity [20].

Liposomes TP1 and TP2 were loaded with a natural antioxidant: chlorophyll *a*, hence the antioxidant nature of these samples. The more antioxidative behavior of TP1 as compared to TP2 is due to more lipid lamellae of TP1 acting as protective layers against oxidative degradation.

The best antioxidant samples proved to be the CNT-based hybrids originating from multilamellar lipid vesicles (TP3), because they are more dispersed than TP4 (see AFM analysis), offering an increased surface area, thus providing more reaction centers that could enhance the capacity of ROS scavenging.

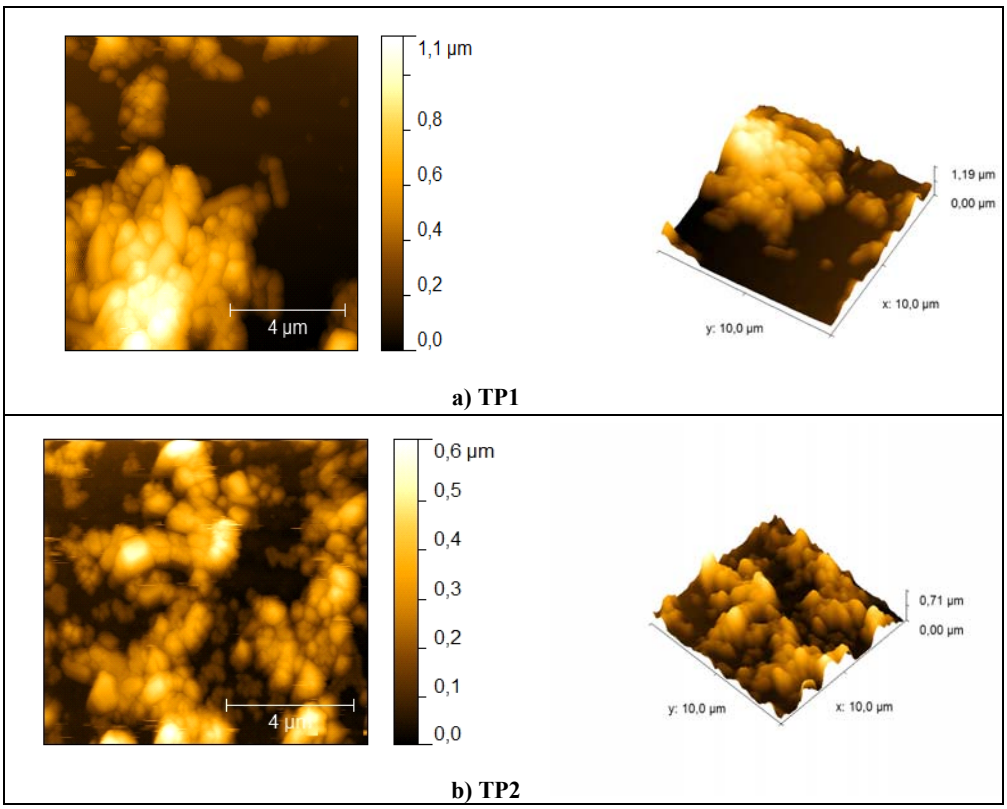

Fig. 1

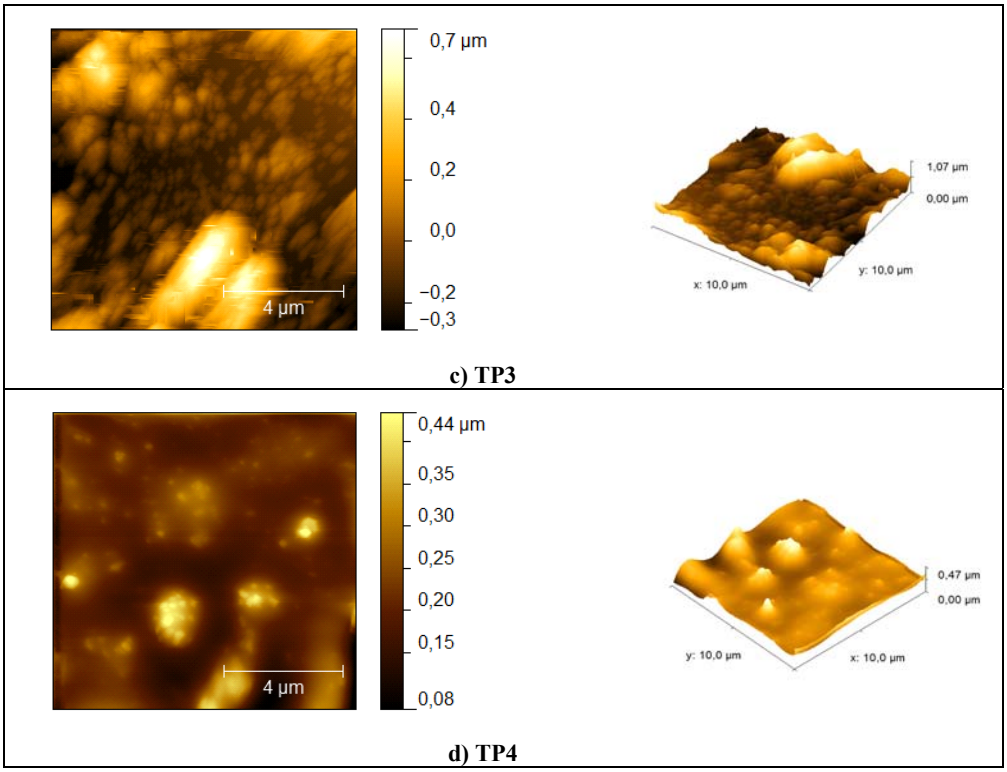

Fig. 1 (continued) – Two (left) and three (right) dimensional AFM images of the samples.

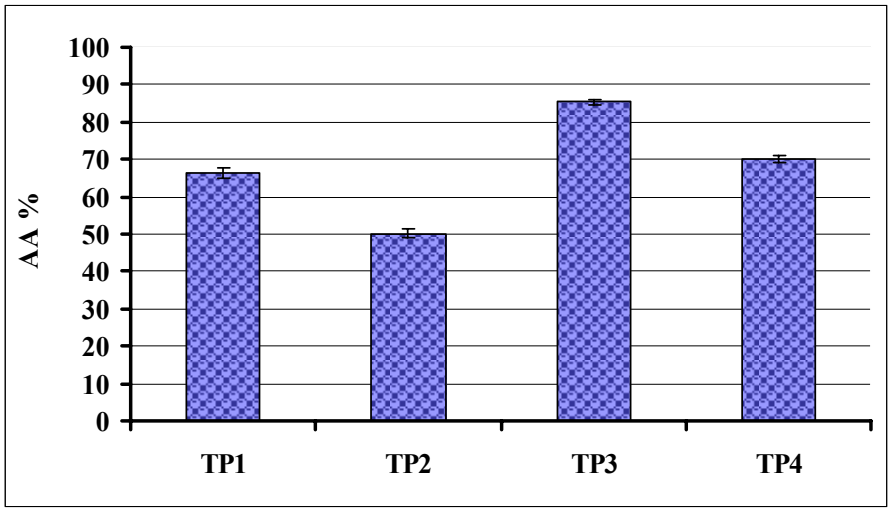

Fig. 2 – The antioxidant activities of the samples.

3.3. ANTIMICROBIAL INVESTIGATIONS

The antimicrobial investigations were performed on *Staphylococcus aureus* ATCC 25923 bacteria using the phosphate buffer solution pH 7.4 as a negative control. This Gram-positive bacterium was chosen in our study because it is a common cause of various severe diseases (skin infections, respiratory diseases, food poisoning) [21].

Figure 3 shows the antimicrobial activities as area of inhibition zone (A_{IZ}) of each sample, against *S. aureus*. Both types of liposomes displayed weak antimicrobial activity, with close values of areas of inhibition zone of 22 and 27 mm^2 for TP1 and TP2, respectively.

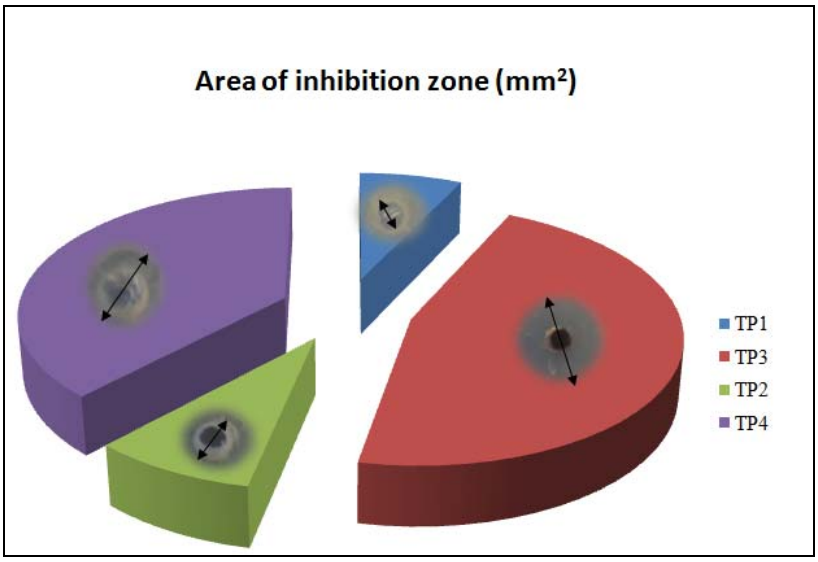

Fig. 3 – Antimicrobial activities (area, in mm^2 of inhibition zone) of the samples, against *Staphylococcus aureus* ATCC 25923.

The CNT-based materials presented the most biocidal effect, more potent proved to be the sample TP3 (A_{IZ} = 143 mm^2) due to their good dispersion state, as compared to TP4 biohybrid (A_{IZ} = 118 mm^2).

The principal mechanism of antimicrobial action of these materials is through direct contact to bacteria cell, leading to physical membrane damage, a better dispersion increasing the available surface and thus the exposure to bacterial contaminants [22, 23]. Sean *et al.* [24] pointed out that the antimicrobial properties of SWCNT-based nanomaterials are also due to the high aspect ratio and the fibrous structure of SWCNTs.

Bai and co-workers found that SWCNTs can capture bacterial cells, causing cell death through direct physical puncture of cell membranes [25].

In our study, the biohybrids contain a biological component: *the biomimetic membranes* which allow a better contact with bacteria cell, then the artificial lipid bilayers can fuse with bacterial membrane, damaging it. These findings are in agreement with our previous works [5, 6]. The results of antibacterial susceptibility assay show promising evidence for the use of these hybrids as antibacterial coatings.

3.4. PHOTOPHYSICAL ASPECTS OF THE QUERCETIN INSERTION IN BIOCOMPOSITES

Quercetin was inserted in the obtained supramolecular soft materials by adding appropriate aliquots of 20 mM quercetin stock solution (in DMSO) to biocomposite suspensions, making sure that in each case, DMSO concentration (v/v) did not exceed 0.5%, as not to affect the lipid bilayers [10].

Chl*a* loaded in biomimetic membranes was used as a spectral sensor to monitor, at molecular level, the flavonoid insertion in the samples. The fluorescence emission spectra of carbon-based hybrids (Fig. 4) revealed the Chl*a* fluorescence quenching with quercetin addition.

For both biocomposites, a linear Stern-Volmer dependence has been obtained by plotting the relative intensity ratio *versus* the quercetin (Q) concentration (Fig. 4): $I_0/I = 1 + K_q \cdot \tau_0 \cdot [Q] = 1 + K_{SV}[Q]$, where: I_0 and I are the steady-state fluorescence intensities in the absence and in the presence of quencher, respectively; $K_{SV} = K_q\tau_0$ is the Stern-Volmer constant; τ_0 is the fluorescence lifetime in the absence of the quercetin; $[Q]$ is the quencher (quercetin) concentration; K_q is the bimolecular quenching constant [26].

According to Lakowicz [26], a linear Stern-Volmer plot is an indicative of a single class of fluorophores, all equally accessible to quencher. Considering $\tau_0 = 4.9$ ns [26] for both Chl*a* in biohybrids, the values of bimolecular quenching constants K_q were $1.109 \cdot 10^{12}$ $M^{-1}s^{-1}$ and $1.45 \cdot 10^{12}$ $M^{-1}s^{-1}$ for TP3 and TP4, respectively, then a static process could be rather considered as responsible for Chl*a* quenching by quercetin, because a dynamic quenching process is characterized by K_q constants in the range of 10^9–10^{10} $M^{-1} \cdot s^{-1}$ [28].

Chl*a* was sensing the changes in the environment of its porphyrin ring, when quercetin was added to biohybrids. The obtained bimolecular quenching constants are close to the values (2.3–2.6) × 10^{11} $M^{-1} \cdot s^{-1}$ reported by Ricchelli [29] for porphyrins freely dissolved in aqueous solutions, suggesting that the Chl*a* molecules accessible to the flavonoid quencher are located in the outer lipid layer, exposed to the aqueous solvent, findings which are consistent with our previous studies [10]. Quercetin inserted in artificial lipid bilayers in biohybrids, between lipid polar heads, at lipid/water interface, similar to chlorophyll. The values of K_q for both biocomposites are much higher than that obtained for liposomes alone ($\sim 7 \cdot 10^{11}$ $M^{-1} \cdot s^{-1}$) in a previous work [10], indicating the presence of CNTs results in increasing in the bimolecular quenching constant values, therefore accentuating

the quercetin insertion in artificial lipid bilayers. This is a benefic effect in terms of some therapeutic applications, knowing that this flavonoid acts as a strong antioxidant and have many biomedical applications.

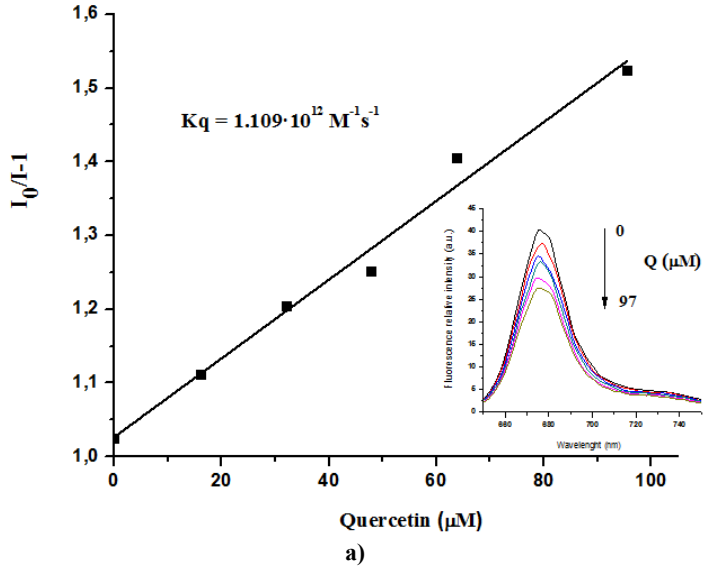

a)

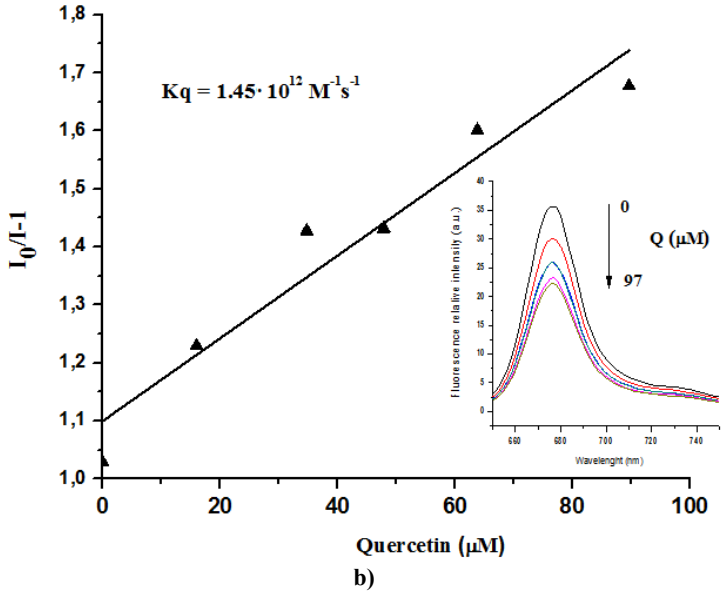

b)

Fig. 4 – Stern-Volmer plots for Chl*a* incorporated in carbon-based biocomposites: TP3 (a) and TP4 (b), quercetin (*Q*) acting as a quencher. In the inset is presented the Chl*a* fluorescence quenching as a function of *Q* concentration.

4. CONCLUSIONS

This paper presents a simple bottom-up approach to obtain biohybrids designed from carbon nanotubes decorated with chlorophyll *a*-loaded bio-inspired membranes. Chl*a* proved to be an excellent optical sensor for monitoring insertion of quercetin in these bio-based composites. Taking into account the antioxidant properties and also the bio-active effect of the prepared CNT-based biocomposites against *Staphylococcus aureus* bacteria, these hybrids could be used in biomedical field or as surface coating materials to prevent bacterial biofilm formation.

The fluorescence studies of the insertion of quercetin in biocomposites based on carbon nanotubes and chlorophyll-loaded biomimetic membranes, open new perspectives for using these materials as scaffolds to carry therapeutic agents.

Acknowledgements. The authors wish to thank Dr. Gabriel Baranga from Faculty of Physics, University of Bucharest, Romania, for performing some fluorescence experiments.

REFERENCES

1. C. C. Ciobotaru, C. M. Damian, S. Polosan, E. Matei, H. Iovu, Dig. J. Nanomater. Bios. **9**(1), 413-422 (2014).
2. C. Nichita, I. Stamatin, Dig. J. Nanomater. Bios. **8**(1), 445-455 (2013)
3. L. Baschir, E. Fagadar-Cosma, I. Creanga, A. Palade, A. Lascu, M. Birdeanu, D. Savastru, V. Savu, S. Antohe, A. Velea, G. Fagadar-Cosma, M. Popescu, I. D. Simandan, Dig. J. Nanomater. Bios. **9**(2), 847-857 (2014).
4. L. Baschir, S. Antohe, A. Radu, R. Constantineanu, S. Iftimie, I. D. Simandan, M. Popescu, Dig. J. Nanomater. Bios. **8**(4), 1645-1651 (2013).
5. M. E. Barbinta-Patrascu, C. Ungureanu, S. M. Iordache, A. M. Iordache, I. R. Bunghez, M. Ghiurea, N. Badea, R. C. Fierascu, I. Stamatin, Mat. Sci. Eng. C **39**, 177-185 (2014).
6. M. E. Barbinta-Patrascu, S. M. Iordache, A. M. Iordache, N. Badea, C. Ungureanu, Beilstein J. Nanotechnol. **5**, 2316-2325 (2014).
7. M. Badran, Dig. J. Nanomater. Bios. **9**(1), 83-91 (2014).
8. P. K. Ang, M. Jaiswal, C. Haley, Y. X. Lim, Y. Wang, J. Sankaran, A. Li, C. T. Lim, T. Wohland, O¨. Barbaros, K. P. Loh, ACS NANO **4**(12), 7387-7394 (2010).
9. M. E. Barbinta-Patrascu, C. Ungureanu, I. Rau, Mol. Cryst. Liq. Cryst. **604**(1), 1-10 (2014).
10. S. Milenkovic, M. E. Barbinta-Patrascu, G. Baranga, D. Markovic, L. Ţugulea, Gen. Physiol. Biophys. **32**, 559-567 (2013).
11. H. H. Strain, W. A. Svec, *The chlorophylls* (Eds. L. P. Vernon and G. R Seely), Academic Press, New York, 1966, p. 21.
12. C. Iancu, C.G. Chilom, *Discovering photosynthesis by experiments*, Rom. Rep. Phys. **68**, 1259-1269 (2016).
13. M. E. Barbinta Patrascu, N. Badea, L. Tugulea, A. Meghea, Key Eng. Mater. **415**, 29-32 (2009).
14. J. A. Ross, C. M. Kasum, Annu. Rev. Nutr. **22**, 19-34 (2002).
15. K. E. Heim, A. R. Tagliaferro, D. J. Bobilya, J. Nutr. Biochem. **13**, 572-584 (2002).
16. B. Pawlikowska-Pawlęga, K. Trębacz, E. Król, A. Gawron, Acta Physiol. Plant. **22**(1), 61-67 (2000).
17. G. Niculae, I. Lacatusu, N. Badea, R. Stan, B. S. Vasile, A. Meghea, Photochem. Photobiol. Sci. **13** (4), 703-716 (2014).

18. I. Lacatusu, N. Badea, R. Nita., M. Giurginca, D. Bojin, I. Iosub, A. Meghea, J. Phys. Org. Chem. **22**, 1015-1021 (2009).
19. G. More, T. E. Tshikalange, N. Lall, F. Botha, J. J. M. Meyer, J. Ethnopharmacol. **119**, 473-477 (2008).
20. I. Fenoglio, M. Tomatis, D. Lison, J. Muller, A. Fonseca, J. B. Nagy, B. Fubini, Free Radic. Biol. Med. **40**, 1227-1233 (2006).
21. A. Ogston, Rev. Infect. Dis. **6** (1), 122-128 (1984).
22. A. Li, L. Wang, M. Li, Z. Xu, P. Li, Z. Z. Zhang, Dig. J. Nanomater. Bios. **9**(2), 599-607 (2014).
23. S. Kang, M. S. Mauter, M. Elimelech, Environ. Sci. Technol. **43**, 2648-2653 (2009).
24. S. C. Smith, D. F. Rodrigues, Carbon **91**, 122-143 (2015).
25. Y. Bai, I. S. Park, S. J. Lee, T. S. Bae, F. Watari, M. Uo, M. H. Lee, Carbon **49**, 3663-3671 (2011).
26. J. R. Lakowicz, *Principles of Fluorescence Spectroscopy*, Plenum Press, New York, 1983.
27. G. Picard, G. Munger, R. M. Leblanc, R. Le Sage, D. Sharma, A. Siemiarczuk, J. R. Bolton, Chem. Phys. Letters **129**, 41-47 (1986).
28. B. Valeur, J. C. Brochon, *New Trends in Fluorescence Spectroscopy: Applications to Chemical and Life Sciences*, Springer, New York, 2001.
29. F. Ricchelli, Biochim. Biophys. Acta **1065**, 42-48 (1991).